J Musculoskelet Neuronal Interact 2020; 20(4):579-590

Journal of Musculoskeletal and Neuronal Interactions JMNI

Original Article

Divergent effects of peripheral and global neuropeptide Y deletion

Natalie K.Y. Wee[1], Ivana Vrhovac Madunic[1,2], Tonci Ivanisevic[1,3], Benjamin P Sinder[1], Ivo Kalajzic[1]

[1]Department of Reconstructive Sciences, University of Connecticut Health Center, Farmington, USA; [2]Molecular Toxicology Unit, Institute for Medical Research and Occupational Health, Zagreb, Croatia; [3]Department of Biochemistry, University of Oxford, Oxford, UK

Abstract

Objectives: Neuropeptide Y (NPY) is involved in the coordination of bone mass and adiposity. However, multiple NPY sources exist and their individual contribution to the skeleton and adiposity not known. The objectives of our study were to evaluate the effects of peripheral mesenchymal derived NPY to the skeleton and adiposity and to compare them to the global NPY^{KO} model. **Methods:** To study the role of mesenchymal-derived NPY, we crossed conditional NPY ($NPY^{fl/fl}$) mice with Prx1cre to generate $PrxNPY^{KO}$ mice. The bone phenotype was assessed using micro-CT. The skeletal phenotype of $PrxNPY^{KO}$ mice was subsequently compared to global NPY^{KO} model. We evaluated body weight, adiposity and functionally assessed the feeding response of NPY neurons to determine whether central NPY signaling was altered by Prx1cre. **Results:** We identified the increase in cortical parameters in $PrxNPY^{KO}$ mice with no changes to cancellous bone. This was the opposite phenotype to global NPY^{KO} mice generated from the same conditional allele. Male NPY^{KO} mice have increased adiposity, while $PrxNPY^{KO}$ mice showed no difference, demonstrating that local mesenchymal-derived NPY does not influence adiposity. **Conclusion:** NPY mediates both positive and negative effects on bone mass *via* separate regulatory pathways. Deletion of mesenchymal-derived NPY had a positive effect on bone mass.

Keywords: Adipocyte, Cortical Bone, Mesenchymal Cells, Neuropeptide Y, Osteoblast

Introduction

Local factors that regulate osteoblasts and osteocytes are potential targets for therapeutic application to improve bone mass. Neuropeptide Y (NPY) is a 36 amino acid neurotransmitter, once secreted has a half-life of approximately 4 minutes[1]. Our previous studies have identified a 9-fold enrichment of NPY mRNA in dentin matrix protein 1 (DMP1) expressing osteocytes in comparison to Col2.3 osteoblasts, thus showing that osteocytes are a predominant source of local NPY expression[2]. We have identified local expression of NPY within different populations of bone cells: calvarial osteoblasts, bone marrow stromal cells and bone marrow mononuclear cells[3]. Calvarial osteoblasts upregulate NPY-Y1 receptor expression during differentiation; and thus are the primary target cells for NPY in bone[3]. We have previously demonstrated that global deletion of NPY (NPY^{KO}) had a perplexing phenotype with reduced bone cross-sectional area and reduced mechanical strength. Nevertheless, the direct *in vitro* effects on bone marrow stromal cells (BMSCs) showed that NPY deficiency improves differentiation and mineralization[3]. Thus, these results led to the hypothesis that there may be multiple distinct NPY pathways regulating skeleton.

Energy metabolism is another physiological system on which NPY signaling has potent effects[4-6]. The NPY effects have predominantly been observed in Y receptor knockout mice. While the increase of NPY is known to greatly increase appetite leading to increased adiposity[7], the metabolic phenotype of global NPY deficiency was initially underwhelming, as there were no observed differences in body weight or food intake, only differences in their leptin

The authors have no conflict of interest. This work has been supported by NIH/NIAMS grants AR055607, AR070813-and Research Excellence Program funds by UConn to I.K.

Corresponding author: Ivo Kalajzic, Department of Reconstructive Sciences, MC 3705, School of Dental Medicine, UConn Health, 263 Farmington Ave, Farmington, CT 06030, USA
E-mail: ikalaj@uchc.edu

Edited by: G. Lyritis
Accepted 4 July 2020

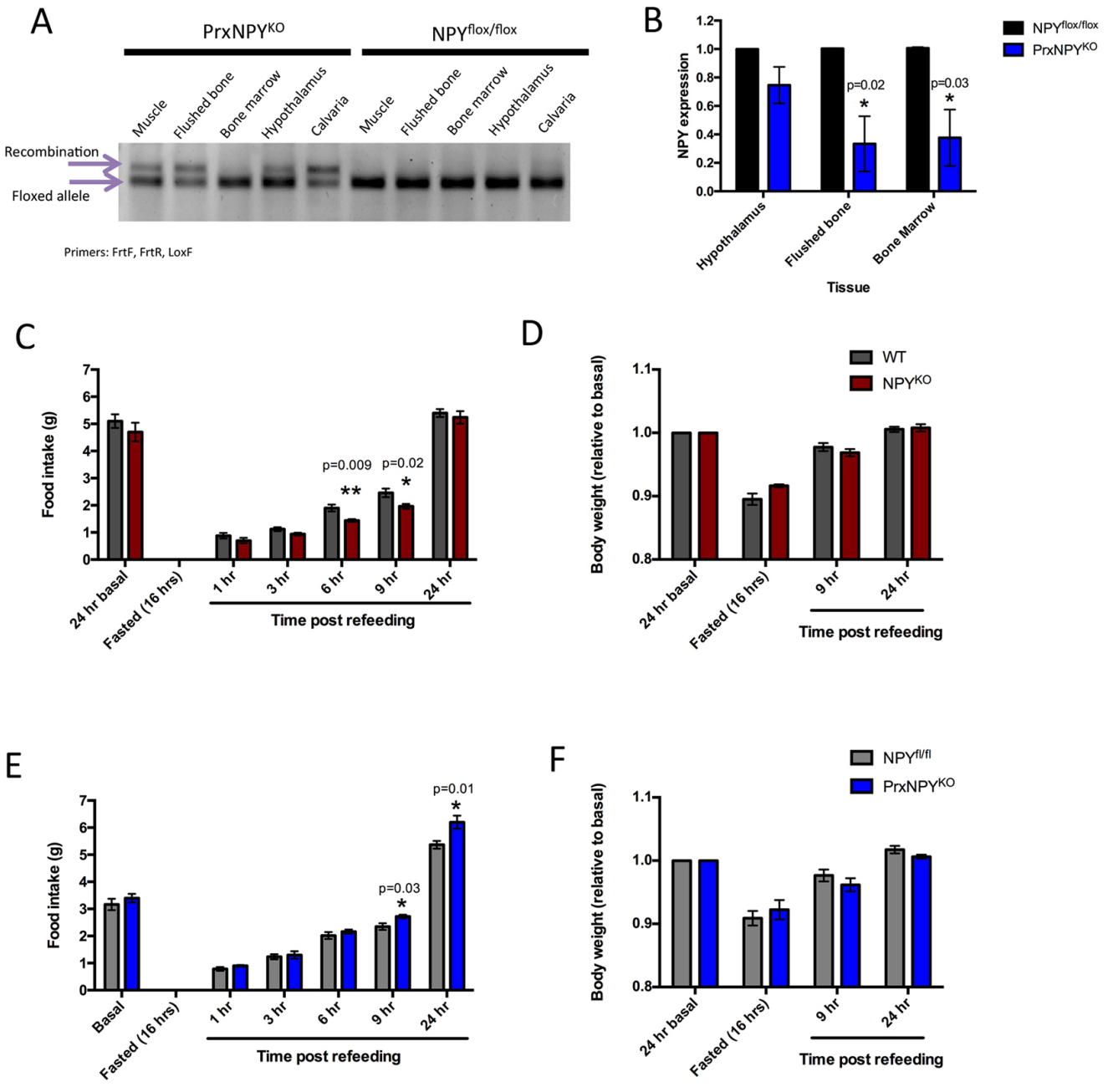

Figure 1. Generation of PrxNPY model. A. DNA Recombination of NPY allele is evident in PrxNPY^{KO} mice; PrxNPY^{KO} n=3; NPY$^{fl/fl}$ n=3. **B.** NPY transcript is reduced in bone and bone marrow cells but not in hypothalamus; n=3. **C.** Food intake in grams of PrxNPY mice during fast-induced food intake study. **D.** Body weight of PrxNPY^{KO} mice during fast-induced food intake. **E.** Food intake in grams of NPY^{KO} mice during fast-induced food intake study. **F.** Body weight of NPY^{KO} mice during fast-induced food intake. **(C, D)**: PrxNPY^{KO}: n=6. NPY$^{fl/fl}$: n=5. **(E, F)**: WT: n=5. NPY^{KO}: n=5. Statistical analyses: Student's t-tests (B) and Student' s t-tests with an adjustment for multiple comparisons (C-F). *p<0.05; **p<0.01.

sensitivity[8]. Subsequent studies that backcrossed the same mice to a C57Bl/6 background identified that the mice developed a mild obesity and had impaired re-feeding responses[9,10]; demonstrating that the genetic background was important for examining the role of NPY in energy metabolism and adiposity. Similarly, we identified that our global NPY^{KO} mouse on a C57Bl/6J background had increased adiposity[3].

The development of NPY specific deletions will assist in identifying the sources of NPY and their contributions to peripheral tissues. The aims of this study were to evaluate the effects of peripheral mesenchymal derived NPY to the

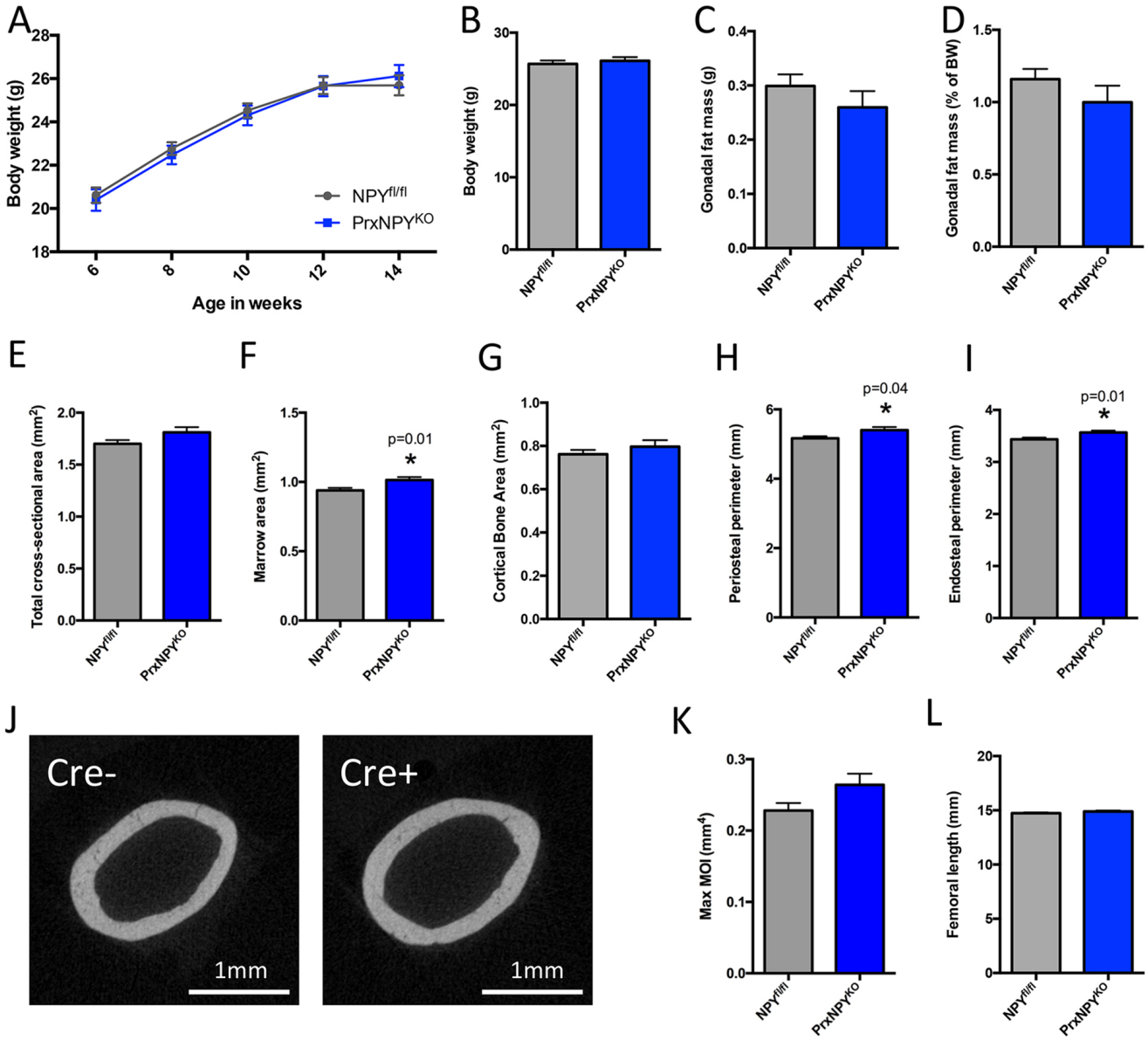

Figure 2. Local deletion of NPY increases bone size in 14-week old male mice. **A.** Body weight from 6 to 14 weeks of age. **B.** Body weight at 14 weeks of age. **C.** Gonadal fat pad weight. **D.** Gonadal fat pad weight expressed as a percentage of body weight. MicroCT analysis of PrxNPY^{KO} bones: **E.** Total bone area, **F.** Marrow area, **G.** Cortical bone area, **H.** Periosteal perimeter, **I.** Endosteal perimeter, **J.** Representative cortical cross-sections. **K.** Maximum moment of inertia (MOI) and **L.** Femur length. PrxNPY^{KO} n=11; NPY$^{fl/fl}$ n=12. Statistical tests: two-way repeated measures ANOVA (A) and Students t-tests (**B-I, K, L**). *p<0.05.

skeleton and adiposity using Prx1cre, and to compare this to our global NPY^{KO} model.

Material and Methods

Mouse strains and colony management

All procedures were approved by the UConn Health Institutional Animal Care and Use Committee and performed in an AAALAC accredited facility. Mice were group housed in ventilated cages with a 12 h light cycle (7 am - 7 pm). The room temperature was maintained at 22°C. Water and irradiated rodent chow (Teklad 2918, Invigo, Indianapolis, IN) was provided *ad libitum*. NPY$^{fl/fl}$ and NPY^{KO} models have been previously described[3]. Briefly, we inserted a loxP site between Exon 1 and Exon 2 and an Frt-loxP site between Exon 3 and Exon 4 using CRISPR to flank all but two protein-coding amino acids and then crossed our model to either *Hprt*-cre to generate global knockout (NPY^{KO}) or Prx1cre[11] to generate a peripheral mesenchymal specific model (PrxNPY^{KO}). PrxNPY^{KO} mice were consistently bred such that

the male breeder harbored the Cre allele, to ensure that global recombination did not occur as previously reported by Logan, Martin[11]. Genotyping was done as previously described for NPY flox allele[3] and Cre[12]. To check for recombination in the PrxNPY^{KO} model, DNA was extracted from muscle, flushed bone, bone marrow, hypothalamus and calvarial tissues. RNA extraction and real time PCR were done to confirm RNA depletion[3]. Both sexes of mice were evaluated for bone phenotypes, the sex used is indicated in the figure legends.

Fast-induced food intake

At 8 weeks of age, mice were single housed and acclimatized for 24 hrs prior to food monitoring. Basal food intake was measured as the amount of food consumed in 24 hrs. Following this, mice were fasted for a 16 hr period starting at 5 pm. At 9 am, the mice were given food and the amount of food consumed was recorded at intervals for 24 hrs to examine the response of re-feeding following fasting. Body weight was also recorded at the beginning, prior to fasting, after fasting and on completion of the experiment.

Tissue collection

Samples were collected at 14 and 24 weeks of age. Femurs were fixed in 4% paraformaldehyde (PFA) and stored in phosphate buffered saline PBS for microCT, then transferred to 30% sucrose and frozen at -20°C prior to cryo-embedding. Tibias were fixed in 4% PFA. The following organs and tissues were dissected free and weighed: liver, pancreas, kidney, spleen, seminal vesicles, brown adipose tissue (BAT), inguinal white adipose tissue (iWAT), epididymal WAT (eWAT), retroperitoneal WAT (rWAT) and mesenteric (mWAT).

MicroCT

Femurs were assessed using cone beam micro-focus X-ray computed tomography (μCT40, Scanco Medical AG, Switzerland). Three-dimensional 16-bit grayscale images were reconstructed using standard convolution back-projection algorithms with Shepp and Logan filtering, and rendered within an 8 mm field of view at a discrete density of 16384 voxels/mm^3 (isometric 8 μm voxels). Segmentation of bone was performed with a constrained Gaussian filter to reduce noise, applying standardized thresholds for trabecular and cortical bone, respectively. Trabecular morphometry was measured in the distal femur metaphysis, defining a volumetric region of interest within the endocortical surface of a 1 mm span referenced 1 mm from the growth plate. Cortical bone morphometry was measured within a 600 μm span, referenced 5.1 mm from the growth plate.

Perilipin staining and BMAT analysis

Perilipin staining was performed as previously described[13]. Briefly, post-fixation, femurs or tibiae were decalcified using 0.5M EDTA for a week with solution changed every 2 days. Then samples were placed in 30% sucrose for 48 hrs prior to cryoembedding. The sections were permeabilized in PBS with 0.3% Triton X-100, blocked with 10% normal donkey serum, incubated with anti-Perilipin antibody (Cat#: GP29, American Research Products; 1:500) overnight, rinsed, incubated with secondary antibody donkey anti-guinea pig A647 (Cat#: 706-605-148, Jackson Immunoresearch; 1:250) for 1h at room temperature and mounted in 50% glycerol with DAPI. Images were captured under a Zeiss microscope with an AxioCam MRc camera and Zen software (Zeiss). In a separate experiment, 8-week-old NPY^{KO} mice were fed rosiglitazone diet. Rosiglitazone was commercially mixed with standard Teklad rodent diet (Dosage: 20 ± 2mg/kg/day). Rosiglitazone is a peroxisome proliferator-activated receptor-gamma agonist, known to stimulate bone marrow adipogenesis for a period of 3 weeks and similarly processed as described above. Images were analyzed using FIJI[14], the cancellous region next to the growth plate was evaluated spanning the entire width of the section and was 2 mm in height. The bone marrow area, marrow adiposity along with adipocyte number and size were measured.

Statistical tests

Statistical analyses were performed using Prism 6 (GraphPad software, CA, USA). All data were expressed as means ± standard error of the mean (SEM). Differences between groups were assessed by t-tests or ANOVAs and followed by post hoc Tukey tests, if applicable. The statistical test used for each graph is stated in the figure legend.

Results

Generation of a peripheral mesenchymal NPY deletion model

To determine effects of local mesenchymal-derived NPY originating from mesenchymal cells; we crossed the conditional NPY mouse with Prx1cre to generate PrxNPY^{KO} mice. NPY$^{fl/fl}$ littermates were used as controls. Prx1cre is known to cause DNA recombination in mesenchymal limb tissues (muscle and bone), the hypothalamus and calvaria[11]. We observed the presence of DNA recombination in PrxNPY^{KO} mice in muscle, flushed cortical bone, hypothalamus and calvaria (Figure 1A). We found that NPY expression was significantly reduced by approximately 70% in both flushed cortical bone samples and bone marrow in PrxNPY^{KO} samples relative to NPY$^{fl/fl}$ samples (Figure 1B).

Central NPY neurons within the arcuate nucleus potently regulate appetite[15]. Since we identified the presence of DNA recombination occurring in the hypothalamus and a non-significant reduction (30%) in NPY expression, we functionally assessed the feeding response of NPY neurons to fast-induced re-feeding to determine if central NPY signaling may be altered by Prx1cre. It has been shown that hypothalamic NPY levels are increased following fasting[16]. Thus, with NPY deficiency in the hypothalamus we expected to observe a blunted re-feeding response similar to what had previously been described[9,10]. The global NPY^{KO} mouse

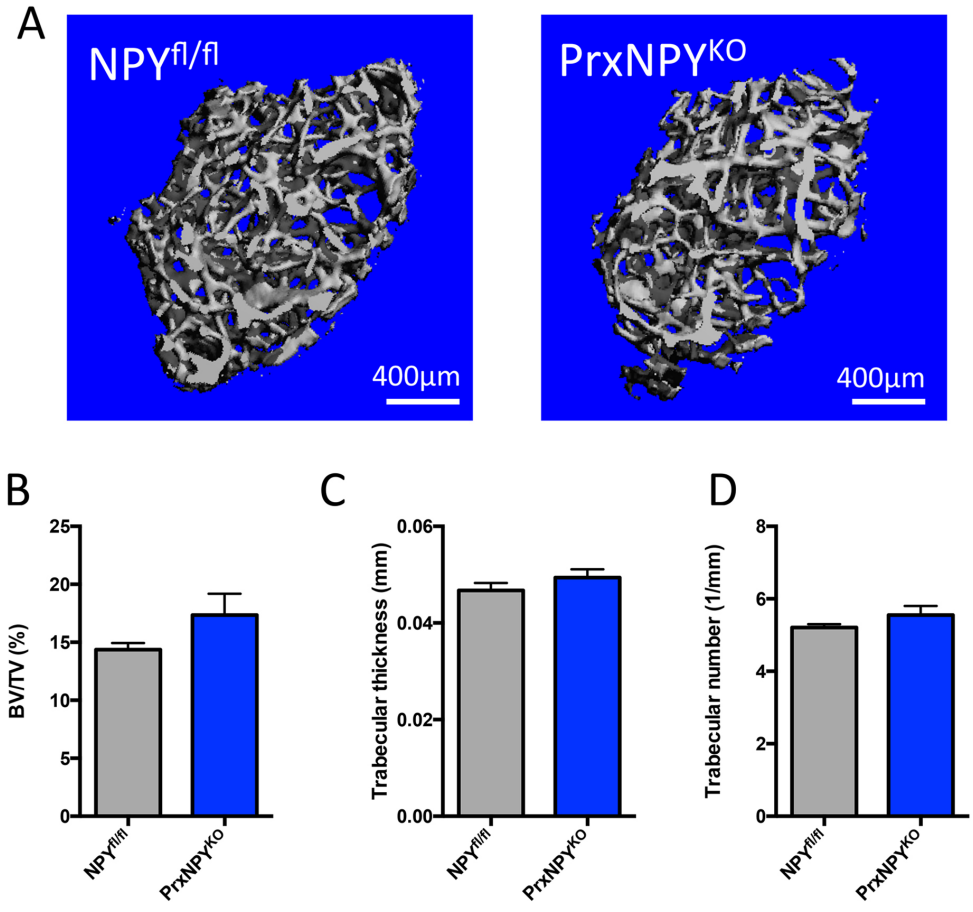

Figure 3. No changes in cancellous bone in 14-week old male PrxNPY^{KO} mice. A. Representative pictures of cancellous bone mass. **B.** Bone volume to tissue volume (BV/TV). **C.** Trabecular thickness and **D.** Trabecular number. PrxNPY^{KO} n=11; NPY$^{fl/fl}$ n=12. Statistical tests: Students t-tests (**B-D**).

consumed less food following fasting (Figure 1C) and their body weight post-fasting was higher in comparison to wild-type (WT) (Figure 1D). We observed PrxNPY^{KO} mice consumed more food during the re-feeding period (Figure 1E) and no differences in body weight during this period (Figure 1F). Thus, we have been able to generate a new model to deplete local NPY production from mesenchymal cells without altering hypothalamic NPY signaling.

Local deletion of NPY improves bone mass in male mice

At 14 weeks of age, male PrxNPY^{KO} mice showed no differences in body weight or adiposity in comparison to NPY$^{fl/fl}$ littermates (Figure 2A-D). However, we identified a trend for increase in total cross-sectional area, marrow area and a significant increase in periosteal perimeter and endosteal perimeters (Figure 2E, F, H, I), indicating that depletion of local NPY increased bone diameter in male mice (Figure 2J). Increases in bone width are known to improve bone strength[17], which was evident by the increased maximum moment of inertia (Figure 2K). Bone length was not altered in response to NPY deletion (Figure 2L). We observed no differences in cancellous bone mass in male PrxNPY^{KO} mice (Figure 3). No change in body weight, adiposity or cortical bone mass was evident in female PrxNPY^{KO} mice (Supplemental Figure 1).

Global and peripheral NPY deletion have opposing effects on bone mass in male mice

Male global NPY^{KO} has reduced cortical cross-sectional area, reduced periosteal and endosteal perimeters and this led to reduced mechanical strength[3]. To compare the PrxNPY^{KO} male mice with the male NPY^{KO} mice, we expressed each model relative to its wildtype control such that WT=1; a value of 1.2 represents a 20% increase in comparison to WT. When assessing cortical bone parameters, we observed that PrxNPY^{KO} mice had consistently increased bone size whilst NPY^{KO} mice had reduced bone size (Figure 4A-E). Bone length was unaltered in PrxNPY^{KO} mice, but mildly reduced in NPY^{KO} mice (Figure 4F). No significant differences were observed in cancellous bone mass (Figure 4G). Altogether, we have

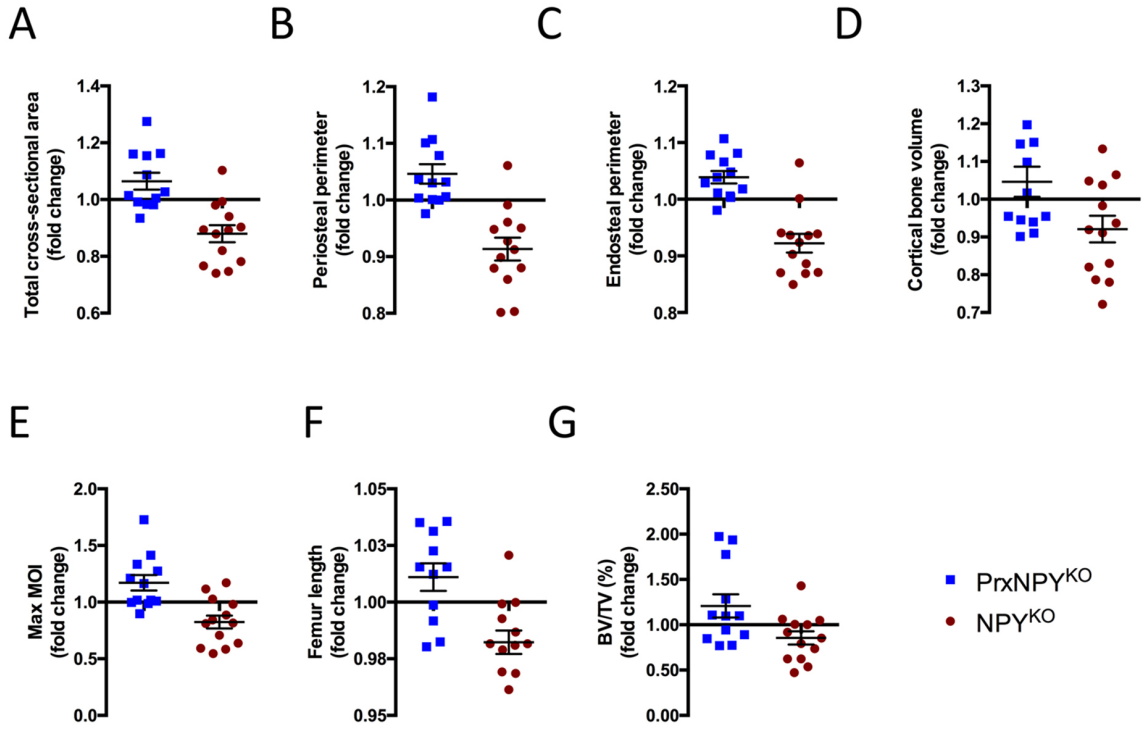

	PrxNPY^{KO}		NPY^{KO}		Relative difference between models
Parameter	**Mean % change from NPY$^{fl/fl}$**	**p-value**	**Mean % change from WT**	**p-value**	
Total cross-sectional area	+7%	0.09	**-12%**	***<0.01****	-19%
Periosteal perimeter	***+5%***	***0.04****	**-9%**	***<0.01****	-14%
Endosteal perimeter	***+4%***	***0.02****	**-8%**	***<0.01****	-12%
Cortical bone volume	+5%	0.36	-8%	0.07	-13%
Max MOI	+17%	0.06	**-17%**	***0.02****	-34%
Femur length	+1%	0.19	**-2%**	***0.03****	-3%
BV/TV	+20%	0.17	-15%	0.11	-35%

Figure 4. Central and peripheral NPY have opposing effects on bone mass in male mice. (**A-G**) Fold change of each model is expressed relative to its respective mean WT. Parameters are as follows: **A**. Total cross-sectional area. **B**. Periosteal perimeter. **C**. Endosteal perimeter. **D**. Cortical bone volume. **E**. Max moment of inertia (MOI). **F**. Femur length. **G**. BV/TV. Data from each model is expressed relative to its control (i.e. =1). NPY^{KO} = 13; WT = 14. PrxNPY^{KO} = 12; NPY$^{fl/fl}$ = 11. Students t-tests were performed on each model with its respective WT to determine if the observed effect was significant. Results are included within the table to show % change (i.e. Mean PrxNPY^{KO}/Mean NPY$^{fl/fl}$ or Mean NPY^{KO}/Mean WT) and statistical analyses.

identified that NPY can mediate both positive and negative effects on bone mass *via* distinct mechanisms in male mice as demonstrated through these models. Female mice from both PrxNPY^{KO} and NPY^{KO} lines showed no differences in cortical bone mass (Supplemental Figure 1) and Wee et al, 2019[3].

PrxNPY mice have no differences in white adipose tissue

Peripheral NPY has been implicated in the regulation of bone and energy[18,19]. However, the direct contribution of NPY to these processes has not been previously examined. We used 6 months old NPY^{KO} and PrxNPY^{KO} mice to assess changes in adipose tissues including bone marrow adipocytes. No changes in body weight or white adipose tissue were present in PrxNPY^{KO} mice. However, increased body weight was evident in NPY^{KO} mice (Figure 5A) and at dissection this was attributed to increases in inguinal (iWAT), epididymal (eWAT), retroperitoneal (rWAT) and mesenteric white adipose depots (mWAT) (Figure 5B). We did not identify any changes in organ weights of liver, pancreas, kidney, spleen, testis or seminal vesicles in PrxNPY^{KO} or NPY^{KO} mice (Table 1). This suggests that the changes in white adipose tissue in the NPY^{KO} are likely attributed to other NPY sources like central regulation and not NPY derived from mesenchymal tissues.

Table 1. Organ and tissue weights at 24 weeks of age.

	PrxNPY		Global NPY^{KO}	
Organ/tissue Weight in grams	**NPY$^{fl/fl}$** (n=6)	**PrxNPY^{KO}** (n=6)	**WT** (n=6)	**NPY^{KO}** (n=5)
Brown adipose tissue	0.09 ± 0.01	0.11 ± 0.01	0.11 ± 0.01	0.09 ± 0.01
Liver	1.43 ± 0.08	1.35 ± 0.06	1.35 ± 0.06	1.34 ±0.05
Pancreas	0.27 ± 0.02	0.30 ± 0.02	0.30 ± 0.02	0.30 ± 0.01
Kidney	0.18 ± 0.01	0.19 ± 0.01	0.19 ± 0.01	0.19 ± 0.01
Spleen	0.07 ± 0.01	0.07 ± 0.01	0.07 ± 0.01	0.08 ± 0.01
Testis	0.10 ± 0.01	0.10 ± 0.01	0.10 ± 0.01	0.11 ± 0.01
Seminal vesicle	0.37 ± 0.01	0.40 ± 0.02	0.40 ± 0.02	0.39 ± 0.01
Mean ± Standard error of the mean				

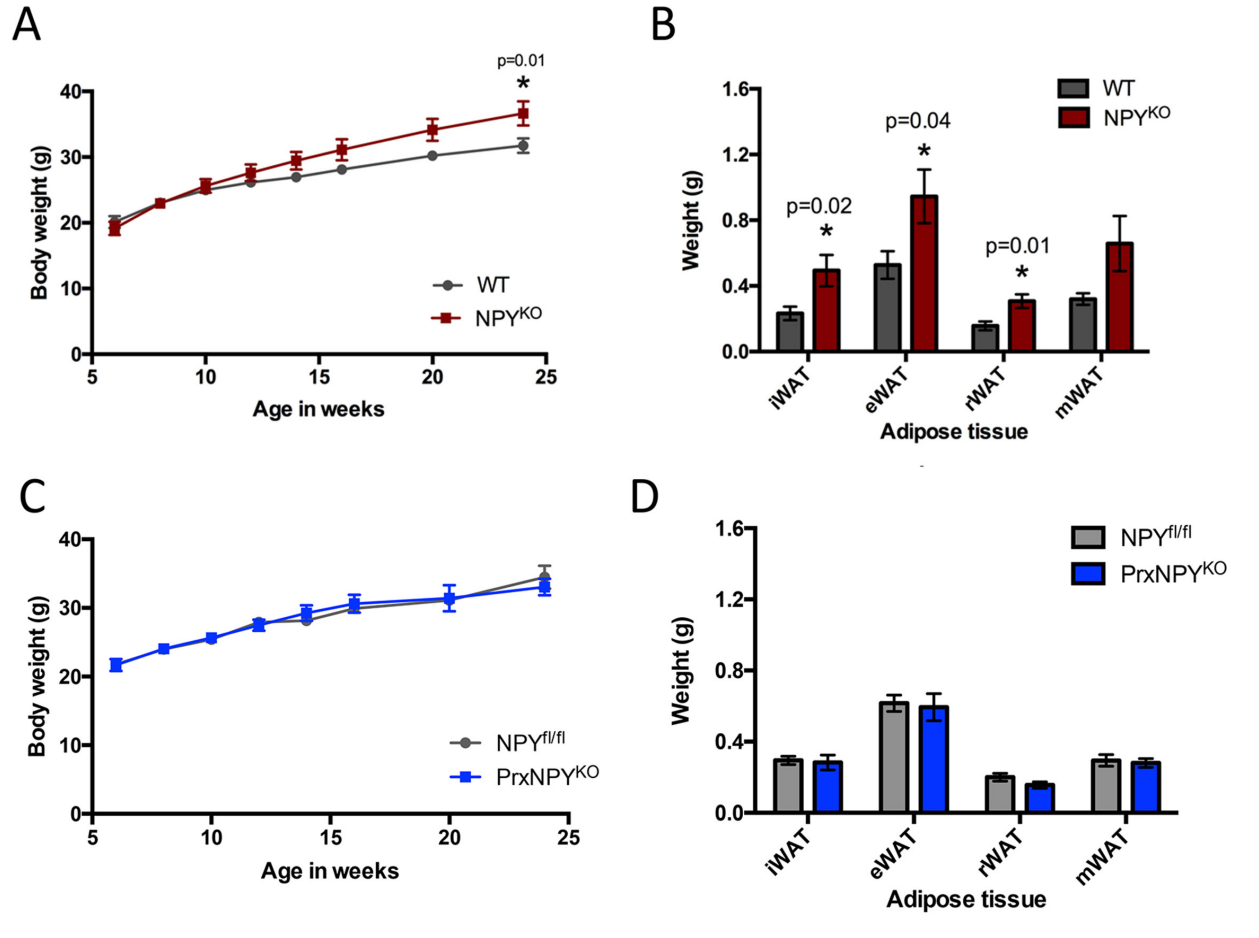

Figure 5. Local NPY does not influence peripheral adiposity in male mice. A. Body weight from 6 weeks to 24 weeks of age of NPY^{KO} mice. **B**. Dissected weight of individual fat pads of NPY^{KO} mice. WT: n=6. NPY^{KO}: n=5. **C**. Body weight from 6 weeks to 24 weeks of age of PrxNPY^{KO} mice. **D**. Dissected weight of individual fat pads of PrxNPY mice. PrxNPY^{KO}: n=6. NPY$^{fl/fl}$: n=6. *p<0.05.

NPY deficiency did not alter bone marrow adipogenesis

The innervation of long bones has been traced to central regions that express NPY[13] and NPY deficiency is reported to reduce bone marrow adipogenesis[20,21]. Since few bone marrow adipocytes were present in the tibiae of NPY^{KO} mice and PrxNPY^{KO} (data not shown), we decided to examine this notion further by stimulating bone marrow adipogenesis. We fed NPY^{KO} mice a rosiglitazone diet to stimulate bone marrow

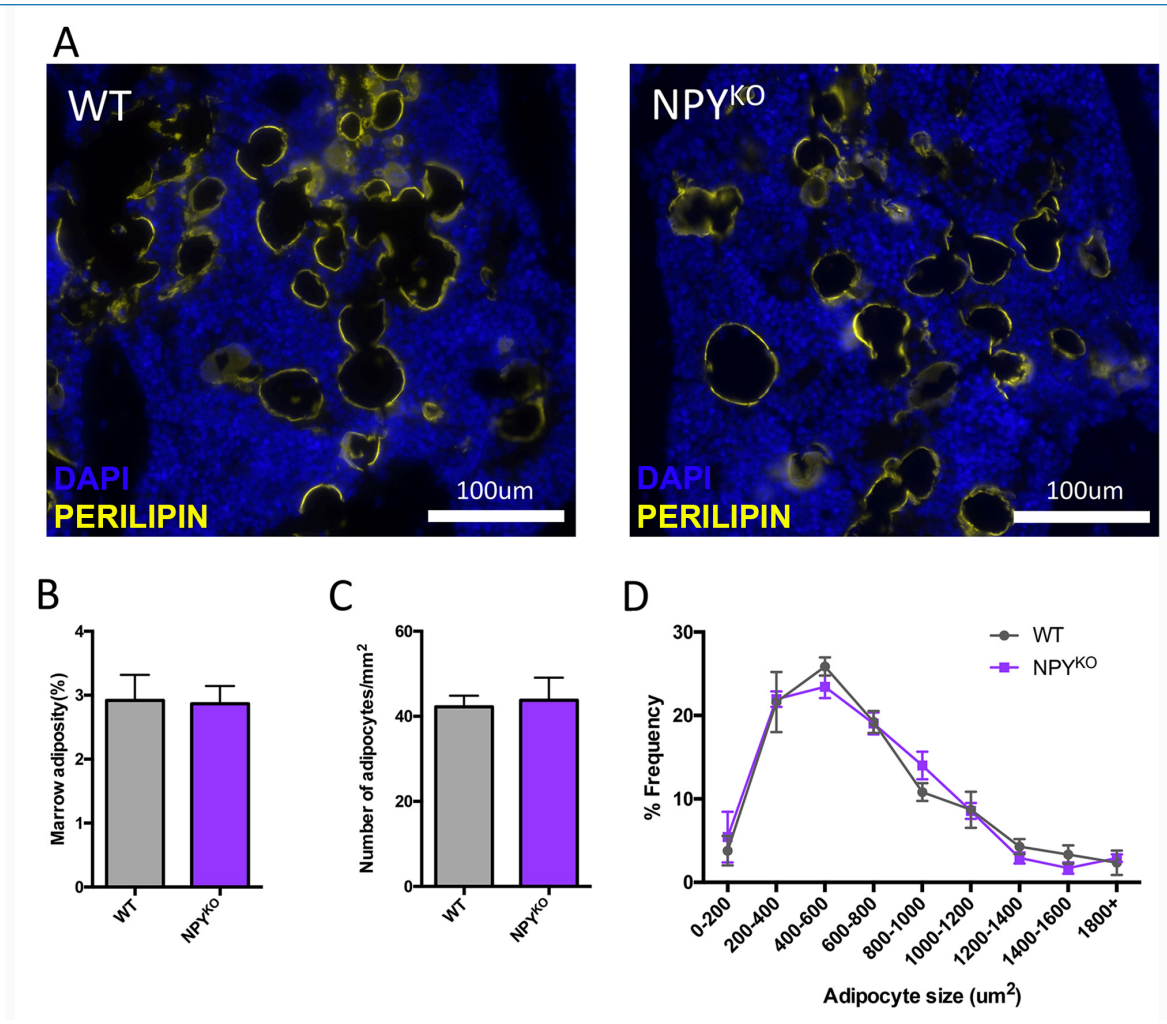

Figure 6. NPY deficiency does not influence BMAT during with rosiglitazone administration. A. Representative images of perilipin staining from WT and NPY^{KO} mice from mice fed rosiglitazone diet. **B**. Percentage marrow adiposity. **C**. Number of adipocytes per mm^2. **D**. Distribution of adipocyte size. **(B-D)** were calculated from perilipin staining. Male mice: WT n=5; NPY^{KO} n=5.

adipogenesis. No difference was evident between WT and NPY^{KO} mice by perilipin staining (Figure 6). Altogether the depletion of endogenous NPY did not alter bone marrow adipogenesis, thus, suggesting that NPY differentially regulates white adipose tissue and bone marrow adipocytes.

Discussion

Neuropeptide Y is expressed in both central and peripheral nervous systems[22]; in addition to local expression within peripheral tissues such as adipocytes[23-25] and bone[2]. Altogether, changes to the NPY system have been shown to influence the brain and peripheral tissues including bone[6,24,26], demonstrating a clear interaction between NPY and bone and energy metabolism (summarized in Figure 7). A large proportion of this work has been gathered from global NPY/Y receptor models, which does not distinguish the effects of specific NPY sources. Work examining NPY signaling within the brain has shown that central NPY can coordinate both bone mass and adiposity[27-30]. However, the direct contribution of mesenchymal-derived NPY to bone mass and adiposity had not been addressed. In this paper, we specifically generated a novel mouse model (PrxNPY^{KO}) to examine the effects of mesenchymal derived NPY to skeletal metabolism.

Using the PrxNPY^{KO} model, we found that peripheral deletion of NPY directly regulates cortical bone, and that multiple distinct NPY pathways exist in the regulation of the skeleton. Specifically, NPY is known to act directly on Y1 receptors on osteoblasts to bone formation (Figure 7); we show that deletion of NPY from osteoblasts and osteocytes using Prx1cre led to an increase in bone size; which is the opposite phenotype observed in the global NPY^{KO} model. Consistent with local NPY deletion, bone-specific Y1 receptor

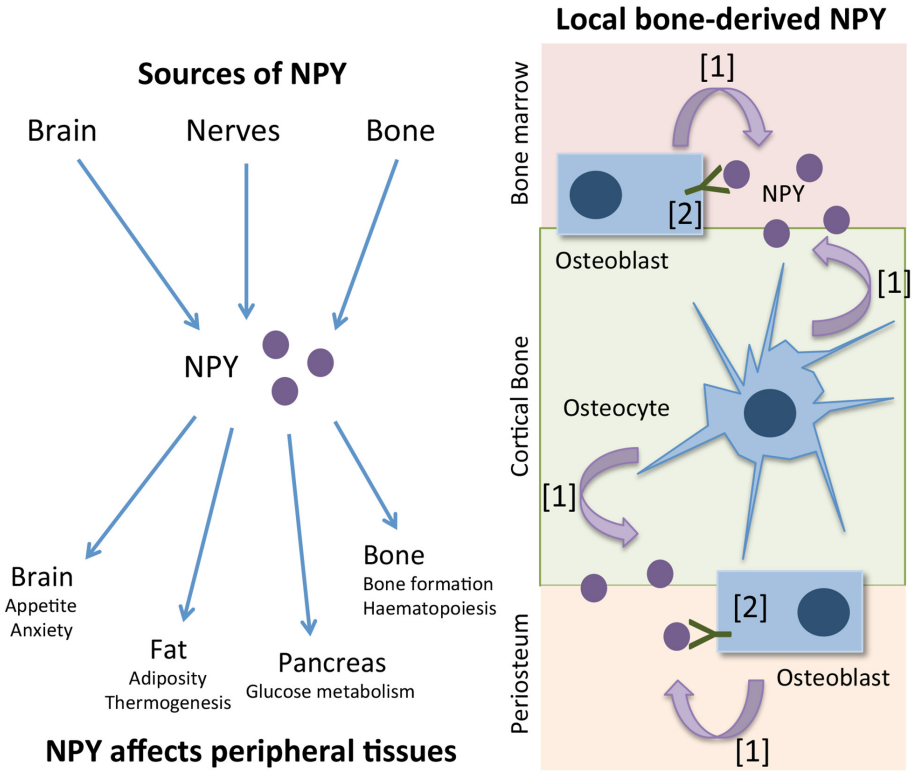

Figure 7. NPY is produced by multiple tissues and exerts effects on a range of tissues (left); local mesenchymal-derived NPY acts in an autocrine/paracrine manner to regulate bone mass (right). [1] Osteoblasts and osteocytes produce NPY. [2] NPY binds to Y1 receptors on osteoblasts and directly inhibiting bone formation.

deficient models have increased bone mass[31,32] and peripheral Y1 antagonism was found to increase the periosteal mineral apposition rate[33]. Y1 deletion and antagonism have greater effects on bone mass since they block central and local NPY sources to the bone. Conversely, local overexpression of NPY under the direction of the Collagen 2.3 promoter reduces cortical bone mass[34]. Excitingly, these data collectively show that targeting peripheral NPY or its Y1 receptor to reduce NPY signaling can improve cortical bone parameters.

Prx1cre is expressed within brain tissue[35], which can make its usage as a peripheral mesenchymal cre controversial when studying neuropeptides. Clear DNA recombination was observed in muscle, flushed bone, the hypothalamus and calvaria but not the bone marrow (Figure 1). Interestingly, NPY RNA expression levels was significantly reduced in bone marrow samples indicating the Prx1cre targeted mesenchymal cells are a major source of NPY within bone marrow. Bone marrow is heterogeneous in its composition including a substantial proportion of hematopoietic cells which are not targeted by Prx1cre. This may explain the absence of DNA recombination present in bone marrow samples. In this study, in addition to checking NPY RNA expression within the hypothalamus, we performed a functional assay examining feeding behavior post fasting, with the assumption that if Prx1cre was targeting NPY neurons then the PrxNPY^{KO} mice would exhibit the same phenotype as NPY^{KO} mice. We observed no reduction in hypothalamic NPY levels and neither did these mice display a blunted re-feeding response, indicating that this particular model only affects NPY in the periphery. Yue et al (2016) also demonstrated by crossing Prx1cre with the very sensitive Ai9 reporter that cre expression was not occurring within hypothalamic neurons[35]. Additionally, Prx1cre is expressed in adipocytes within the subcutaneous white adipose tissue (specifically the inguinal fat pad)[36]. While a two-fold increase in inguinal fat pads was present in global NPY deficiency, no differences were observed in the PrxNPY^{KO} model, suggesting that changes in adiposity are driven by pathways external to white adipose tissue. Consistent with our results, other global NPY^{KO} models have shown an increase in fat mass when bred on a C57Bl/6 background[9,10], this same phenotype is also observed in the global Y1 deficient mouse[23]. Additionally, changes in brain derived NPY signaling have been shown to regulate fat mass[27]. Thus, the increase in fat mass observed in the NPY^{KO} model is likely the culmination of multiple NPY pathways acting on adipose tissue. While our work examines the contribution of peripheral NPY from mesenchymal tissue, it is difficult to know the specific effects of central-

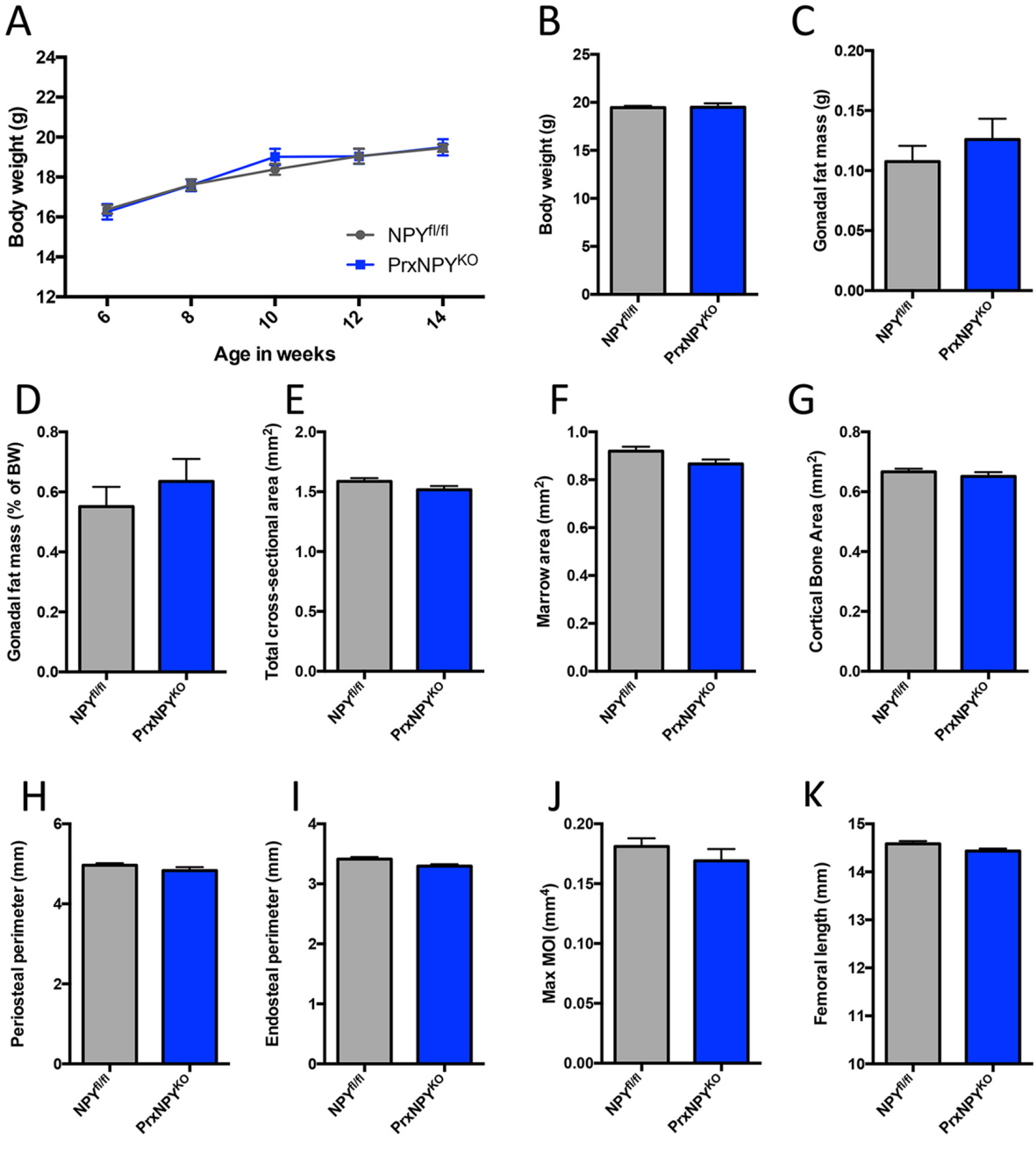

Supplemental Figure 1. Female PrxNPY^{KO} mice have no differences in body weight, adiposity or cortical bone parameters. A. Body weight from 6 to 14 weeks of age. **B**. Body weight at 16 weeks of age. **C**. Gonadal fat pad weight. **D**. Gonadal fat pad weight expressed as a percentage of body weight. MicroCT analysis of PrxNPY^{KO} bones: **E**. Total bone area, **F**. Marrow area, **G**. Cortical bone area, **H**. Periosteal perimeter, **I**. Endosteal perimeter, **J**. Max MOI. **K**. Femur length. NPY$^{fl/fl}$ n=10; PrxNPY^{KO} n=10. Statistical tests: two-way repeated measures ANOVA (A) and Students t-tests (**B-K**).

derived NPY on bone parameters because NPY is produced from several regions of the brain such as the amygdala and hypothalamus and thus may exert multiple effects. One recent study examining neurotensin-expressing neurons in the hypothalamus, showed that NPY deletion significantly reduced cortical bone mass[28]. This phenotype is similar to what we observed in our global NPY^{KO} model[3]. It should be noted that Prx1cre recombination occurs between 9.5- and 10.5-days post conception (dpc), NPY levels have not been examined within mesenchymal cells during embryonic development. Therefore, it is possible that the phenotype observed may be due to compensatory mechanisms that are activated during development.

Secreted factors, derived from bone tissue, influence

feeding behavior and energy metabolism[37-39]. Osteocalcin was the first bone-derived molecule shown to regulate glucose metabolism and adipogenesis by Karsenty and colleagues[37]. More recently, reports indicate sclerostin influences adipose tissue[38] and bone-derived lipocalin 2 suppresses feeding behavior through a melanocortin relay within the hypothalamus[39]. Associations between changes in bone-derived NPY and peripheral adiposity have been drawn[19]. However, this had not been previously assessed by directly deleting NPY from the peripheral skeleton. Our findings suggest that local-derived NPY does not influence white adipose tissue, thus implying that NPY regulation of adiposity is determined by another NPY regulatory pathway, such as those found in the central nervous system.

NPY has been implicated in the regulation of bone marrow adipocytes[20,21]. While we did not observe changes in bone marrow adipocytes in response to NPY deletion when combined with rosiglitazone administration, it is possible that the effect of NPY is context-specific and could be linked to overall changes in whole energy metabolism through indirect mechanisms. Global deletion of the Y1 receptor in combination with leptin deficiency (*ob/ob*) reduced bone marrow adipocytes relative to *ob/ob* controls[40]. While Wang et al. showed with glucocorticoid administration that NPY deficiency reduced PPARγ levels leading to reduced BMAT accumulation and increased bone mass[41]. This suggests that NPY may modulate other pathways that influence BMAT to lead to differential effects.

Conclusion

Altogether, we have shown that NPY regulates skeletal metabolism through distinct mechanisms as peripheral mesenchymal deletion of NPY had opposing effects on cortical bone to that observed in global NPY deletion. We have also identified that NPY differentially regulates white and bone marrow adipocytes and that peripheral mesenchymal deletion of NPY does not influence adiposity.

Acknowledgments

We thank Christian Yon, Erin Wilkie and Christina Dedeo for technical assistance in weaning and genotyping the mice. We thank Dr. Sierra Root for assistance with dissection.

Author contributions

NKW and IK conceived and designed experiments. NKW, IVM, TI, BPS and IK collected the data. NKW and IK interpreted the data. NKW, IVM, TI, BPS and IK participated in drafting the manuscript. NKW wrote the manuscript. NKW, IVM, BPS and IK revised the manuscript. All authors approved the final version of the manuscript.

References

1. Pernow J, Lundberg JM, Kaijser L. Vasoconstrictor effects *in vivo* and plasma disappearance rate of neuropeptide Y in man. Life Sci 1987;40:47-54.
2. Paic F, Igwe JC, Nori R, et al. Identification of differentially expressed genes between osteoblasts and osteocytes. Bone 2009;45:682-92.
3. Wee NK, Sinder BP, Novak S, et al. Skeletal phenotype of the neuropeptide Y knockout mouse. Neuropeptides 2019;73:78-88.
4. Wee NK, Kulkarni RN, Horsnell H, Baldock PA. The brain in bone and fuel metabolism. Bone 2016;82:56-63.
5. Khor EC, Wee NK, Baldock PA. Influence of hormonal appetite and energy regulators on bone. Curr Osteoporos Rep 2013;11:194-202.
6. Loh K, Herzog H, Shi YC. Regulation of energy homeostasis by the NPY system. Trends Endocrinol Metab 2015;26:125-35.
7. Stanley BG, Kyrkouli SE, Lampert S, Leibowitz SF. Neuropeptide Y chronically injected into the hypothalamus: a powerful neurochemical inducer of hyperphagia and obesity. Peptides 1986;7:1189-92.
8. Erickson JC, Clegg KE, Palmiter RD. Sensitivity to leptin and susceptibility to seizures of mice lacking neuropeptide Y. Nature 1996;381:415-21.
9. Segal-Lieberman G, Trombly DJ, Juthani V, Wang X, Maratos-Flier E. NPY ablation in C57BL/6 mice leads to mild obesity and to an impaired refeeding response to fasting. Am J Physiol Endocrinol Metab 2003; 284:E1131-9.
10. Patel HR, Qi Y, Hawkins EJ, et al. Neuropeptide Y deficiency attenuates responses to fasting and high-fat diet in obesity-prone mice. Diabetes 2006;55:3091-8.
11. Logan M, Martin JF, Nagy A, Lobe C, Olson EN, Tabin CJ. Expression of Cre Recombinase in the developing mouse limb bud driven by a Prxl enhancer. Genesis 2002; 33:77-80.
12. Matthews BG, Grcevic D, Wang L, et al. Analysis of alphaSMA-labeled progenitor cell commitment identifies notch signaling as an important pathway in fracture healing. Journal of bone and mineral research: the official journal of the American Society for Bone and Mineral Research 2014;29:1283-94.
13. Wee NK, Lorenz MR, Bekirov Y, Jacquin MF, Scheller EL. Shared Autonomic Pathways Connect Bone Marrow and Peripheral Adipose Tissues Across the Central Neuraxis. Front Endocrinol (Lausanne) 2019;10:668.
14. Schindelin J, Arganda-Carreras I, Frise E, et al. Fiji: an open-source platform for biological-image analysis. Nat Methods 2012;9:676-82.
15. Shi YC, Baldock PA. Central and peripheral mechanisms of the NPY system in the regulation of bone and adipose tissue. Bone 2012;50:430-6.
16. Shi YC, Lau J, Lin Z, et al. Arcuate NPY controls sympathetic output and BAT function via a relay of tyrosine hydroxylase neurons in the PVN. Cell metabolism 2013;17:236-48.
17. Cole JH van der Meulen MC. Whole bone mechanics and bone quality. Clin Orthop Relat Res 2011;469:2139-49.
18. Kaludjerovic J, Ward WE. Bone-specific gene expression patterns and whole bone tissue of female mice are programmed by early life exposure to soy isoflavones

and folic acid. J Nutr Biochem 2015;26:1068-76.
19. Rodriguez-Carballo E, Gamez B, Mendez-Lucas A, et al. p38alpha function in osteoblasts influences adipose tissue homeostasis. FASEB J 2015;29:1414-25.
20. Allison SJ, Baldock PA, Enriquez RF, et al. Critical interplay between neuropeptide Y and sex steroid pathways in bone and adipose tissue homeostasis. Journal of bone and mineral research: the official journal of the American Society for Bone and Mineral Research 2009;24:294-304.
21. Wang FS, Lian WS, Weng WT, et al. Neuropeptide Y mediates glucocorticoid-induced osteoporosis and marrow adiposity in mice. Osteoporos Int 2016; 27:2777-89.
22. Hokfelt T, Broberger C, Zhang X, et al. Neuropeptide Y: some viewpoints on a multifaceted peptide in the normal and diseased nervous system. Brain Res Brain Res Rev 1998;26:154-66.
23. Baldock PA, Allison SJ, Lundberg P, et al. Novel role of Y1 receptors in the coordinated regulation of bone and energy homeostasis. J Biol Chem 2007; 282:19092-102.
24. Kuo LE, Kitlinska JB, Tilan JU, et al. Neuropeptide Y acts directly in the periphery on fat tissue and mediates stress-induced obesity and metabolic syndrome. Nature medicine 2007;13:803-11.
25. Yang K, Guan H, Arany E, Hill DJ, Cao X. Neuropeptide Y is produced in visceral adipose tissue and promotes proliferation of adipocyte precursor cells via the Y1 receptor. FASEB J 2008;22:2452-64.
26. Karl T, Duffy L, Herzog H. Behavioural profile of a new mouse model for NPY deficiency. The European journal of neuroscience 2008;28:173-80.
27. Shi YC, Lin S, Wong IP, et al. NPY neuron-specific Y2 receptors regulate adipose tissue and trabecular bone but not cortical bone homeostasis in mice. PloS one 2010;5:e11361.
28. Lee NJ, Qi Y, Enriquez RF, Ip CK, Herzog H. Lack of NPY in neurotensin neurons leads to a lean phenotype. Neuropeptides 2020;80:101994.
29. Baldock PA, Sainsbury A, Couzens M, et al. Hypothalamic Y2 receptors regulate bone formation. The Journal of clinical investigation 2002;109:915-21.
30. Baldock PA, Sainsbury A, Allison S, et al. Hypothalamic Control of Bone Formation: Distinct Actions of Leptin and Y2 Receptor Pathways. Journal of Bone and Mineral Research 2005;20:1851-7.
31. Lee NJ, Nguyen AD, Enriquez RF, et al. Osteoblast specific Y1 receptor deletion enhances bone mass. Bone 2011;48:461-7.
32. Lee NJ, Nguyen AD, Enriquez RF, et al. NPY signalling in early osteoblasts controls glucose homeostasis. Mol Metab 2015;4:164-74.
33. Sousa DM, Baldock PA, Enriquez RF, et al. Neuropeptide Y Y1 receptor antagonism increases bone mass in mice. Bone 2012;51:8-16.
34. Matic I, Matthews BG, Kizivat T, et al. Bone-specific overexpression of NPY modulates osteogenesis. J Musculoskeletal Neuronal Interact 2012;12:209-18.
35. Yue R, Zhou BO, Shimada IS, Zhao Z, Morrison SJ. Leptin Receptor Promotes Adipogenesis and Reduces Osteogenesis by Regulating Mesenchymal Stromal Cells in Adult Bone Marrow. Cell Stem Cell 2016;18:782-96.
36. Sanchez-Gurmaches J, Hsiao WY, Guertin DA. Highly selective *in vivo* labeling of subcutaneous white adipocyte precursors with Prx1-Cre. Stem Cell Reports 2015;4:541-50.
37. Lee NK, Sowa H, Hinoi E, et al. Endocrine regulation of energy metabolism by the skeleton. Cell 2007; 130:456-69.
38. Kim SP, Frey JL, Li Z, et al. Sclerostin influences body composition by regulating catabolic and anabolic metabolism in adipocytes. Proc Natl Acad Sci U S A 2017;114:E11238-E47.
39. Mosialou I, Shikhel S, Liu JM, et al. MC4R-dependent suppression of appetite by bone-derived lipocalin 2. Nature 2017;543:385-90.
40. Allison SJ, Baldock PA, Enriquez RF, Lin E, During M, Gardiner EM, Eisman JA, Sainsbury A, Herzog H. Critical interplay between neuropeptide Y and sex steroid pathways in bone and adipose tissue homeostasis. J Bone Miner Res. 2009;24(2):294-304.
41. Wang FS, Lian WS, Weng WT, Sun YC, Ke HJ, Chen YS, Ko JY. Neuropeptide Y mediates glucocorticoid-induced osteoporosis and marrow adiposity in mice. Osteoporos Int 2016;27(9):2777-89.